Proceedings of:
ASME TURBO EXPO 2006
May 8-11, 2006, Barcelona, Spain

GT2006-90561

An Experimental Investigation of Secondary Flows and Loss Development Downstream of a Highly Loaded Low Pressure Turbine Outlet Guide Vane Cascade

Johan Hjärne
Department of Applied Mechanics
Chalmers University of Technology
412 96 Gothenburg, Sweden
johan.hjarne@chalmers.se

Valery Chernoray
Department of Applied Mechanics
Chalmers University of Technology
412 96 Gothenburg, Sweden
Valery.chernoray@chalmers.se

Jonas Larsson
Department of Aero and Thermo Dynamics
Volvo Aero Corporation
461 81 Trollhättan, Sweden
jonas.larsson@volvo.com

Lennart Löfdahl
Department of Applied Mechanics
Chalmers University of Technology
412 96 Gothenburg, Sweden
lennart.lofdahl@chalmers.se

ABSTRACT

This paper presents a detailed experimental investigation of the evolution of secondary flow field characteristics and losses at several measurement planes downstream of a highly loaded low pressure turbine/outlet guide vane (LPT/OGV). The experiments were carried out in a linear cascade at Chalmers in Sweden. Several realistic upstream incidences and turbulence intensities have been investigated for one Reynolds number. Downstream characteristics have been measured with a 5-hole pneumatic probe. This allows for the determination of the mean vortical structures, their development and their interactions. The passage vortex and the blade shed vorticity are clearly visible at different downstream positions. Their intensity is shown to be strongly dependent on the inlet flow angle. The turbulence level seems to play a role on both the mixing within, and between the structures. The measurements also show that the losses along the blade span are dependent on the development of these structures.

.

1 INTRODUCTION

Cost and weight requirements on modern jet engines often lead to more highly loaded turbines with fewer stages. In un-geared two and three shaft engines, this gives higher swirl angles into the LPT/OGV and thus makes the aerodynamic design of the OGV more difficult. Structural requirements also lead to non-cylindrical shrouds with complex 3D polygonal shapes and sunken engine-mounts with bumps protruding into the gas channel. This has sparked a renewed interest in design methods and validation cases for 3D OGV flows. Secondary flow intensities are directly related to the loading and therefore to the passage turning. This is more important for turbine cascades than for compressors cascades, since the flow turning for a turbine blade is much higher compared to a typical compressor blade. Most of the literature, if not all, is dedicated to turbine flows and in this paper it is shown that there are differences in the downstream evolution between these types of cascades, mainly due to the lower loading for compressor cascades.

A good literature survey for secondary flows in turbine cascades was written by Sieverding [1] in 1985. The endwall inlet boundary layer impinges on the blade leading edge and rolls up to form a horseshoe vortex with two branches on each side. The pressure side legs, under the influence of the transverse pressure gradient, are directed towards the suction side of the neighboring blade where it interacts with the suction side legs of the horseshoe vortex. The pressure side leg along with the cross flow form the passage vortex The suction side leg lifts up and away from the endwall and orbits around the passage vortex as it is convected downstream. Depending on the interaction strength, a corner vortex develops along the suction side corner. A new highly skewed endwall boundary layer forms downstream and develops the second pressure side leg separation line. The downstream loss distribution is mainly a function of loading, inlet boundary layer characteristics and the downstream distance. In the conclusion, the author insists that besides an increased knowledge of the separation line patterns, more experiments were needed to determine each factor's influence.

Another factor of interest, the turbulence intensity, has been investigated by Gregory-Smith and Cleak [2]. They measured the secondary turbulent kinetic energy development through the cascade under low and high freestream turbulence intensities. Their measurements are of great interest, not only for the determination of the flowfield but also for CFD modeling. Moreover, they pointed out that the inlet turbulence intensity has no major influence on the mean flow development and that it has a limited influence on the gradient of loss evolution through the cascade with the secondary turbulent kinetic energy reaching a maximum close to the blade trailing

edge. For a given loading, the loss level seemed to be directly linked to the integral properties of the inlet boundary layer. Their conclusion concerning the loss evolution was confirmed by Sharma and Buttler [3]. For straight cascades with high aspect ratio (no secondary flow interactions between the end-walls), they provided a correlation based on the inlet boundary layer features and the passage turning angle to estimate the extension of the secondary flows on the suction surface of the trailing edge. As a result of their investigations they were able to obtain a correlation for the total pressure losses.

Secondary flow patterns have been investigated through visualizations by Wang et al. [4] and by means of accurate heat transfer measurements by Goldstein and Spores [5]. They confirmed Sieverding's findings and also added some important features about the development of the secondary flowfield. A horseshoe corner vortex is present beside the usual horseshoe vortex at the leading edge. The suction side leading edge corner vortex is stretched by the acceleration and is lifted up along the suction side, close to the position where the passage vortex interacts with the suction side horseshoe vortex. This leading edge corner vortex remains along the blade surface further downstream whilst the passage vortex separates from the suction side. Visualizations of Kawaï et al. [6] show that the pressure side leading edge corner vortex is most likely to form the pressure side corner vortex.

The aim of this paper is to present the downstream passage secondary flows as well as evaluating the performance with downstream distance of a typical modern highly loaded LPT/OGV. This will be done for a fixed inlet boundary layer height with varying inlet turbulence intensity and flow incidence.

NOMENCLATURE

C	Blade chord [m]
Cp	Pressure coefficient
P_s	Static pressure [Pa]
P_{tot}	Total pressure [Pa]
P_{dyn}	Dynamic pressure based on the inlet velocity [Pa]
P_{fs}	Total pressure outside the downstream wakes [Pa]
Re_c	Reynolds number = UC/ν
Tu	Turbulence intensity [%]
U	Inlet velocity
x	x-coordinate
y	y-coordinate
z	z-coordinate

Greek Symbols

δ_{099}	Boundary-layer height [mm]
ξ	Total pressure losses = $(P_{fs}-P_{tot})/P_{dyn}$

Acronyms

LPT	Low pressure turbine
OGV	Outlet guide vane

2 EXPERIMENTAL SETUP

The linear cascade used for these measurements is an open circuit blower type. A 30 kW fan is used to drive the flow through a diffuser and a flow conditioner (consisting of a honeycomb and three screens with different porosity). The flow is accelerated in a 5:1 contraction before it enters the test section. The test section is built up of four parallel discs, two on each side, with the inner discs constituting the side walls of the 7 OGV's, thus forming the cascade.. The gap between the inner and outer discs is used for sucking out the boundary layers developed in the upstream sections. There is one separate suction system on each side driven by two 7.5 kW motors. The two suction systems can thus be adjusted independently in order to obtain an equal static pressure at the wall on both sides of the test section. This has to be done for each incidence angle that can range from 0 to 52 degrees by rotation of the outer side walls. A more detailed description of the test-facility has been given earlier by Hjärne et al. [7,8]

The grid used for generation of free stream turbulence consisted of 5mm bars with a mesh size of 25mm, thus giving a solidity of 0.31. This grid was placed 450mm upstream of the cascade and parallel to the leading edge plane, see Fig. 1. Besides increasing the turbulence intensity from 0.5% to 5%, the parallel grid has two effects. The positive one is that the inlet turbulence intensity is uniform in front of the cascade. However, as it deflects the flow, the outer side wall inclination had to be adapted so that the inlet incidence remained unchanged.

This OGV was designed to obtain experimental results for the validation of numerical simulations It is a 2D geometry profile which is extended in the span direction (z-direction). The on-design requirement for this vane is to turn an incoming flow field with a flow angle of 30 degrees to an axial outflow whilst minimizing the pressure losses. A typical off-design requirement of LPT/OGV's is that the flow should not separate completely in the range of ±10 degrees incidence from the design point. The cascade geometry data is given in table 1.

The periodicity has been checked and is illustrated in Fig. 2 and Fig. 3. The first one shows the static pressure distribution around the three mid vanes for the on-design case with a turbulence intensity of 5%. The variation from one vane to another is insignificant for both the suction side and the pressure side. The second, also showing very good periodicity, gives the total pressure distribution at midspan 0.8 chord lengths downstream of the trailing edge plane for the same load case. In Fig. 4 the loading for the three different inlet angles is shown. For the highest inlet flow angle the loading can be seen to be very high for the OGV investigated, and as a result the periodicity is not as good as that was seen at the two lower inlet flow angles. This is due to a corner separation between the suction side of the OGV and the endwall which extends towards mid span and thus affects the pressure distribution. It can however be noted that the symmetry of the flow field was still good and is shown in Fig. 4 by the six additional control points positioned at 25% and 75% span on the OGV.

Table 1 Cascade geometry data

Number of vanes	7
Chord length (m)	0.22
Pitch to chord ratio	0.91
Aspect ratio (Span to Chord ratio)	0.91
Inlet Reynolds number	280000
Inlet flow angles (°)	20,30,40
Turbulence intensity (%)	0.5 or 5
Incoming boundary layer height, δ_{099}, (mm)	7.15 - 9.6

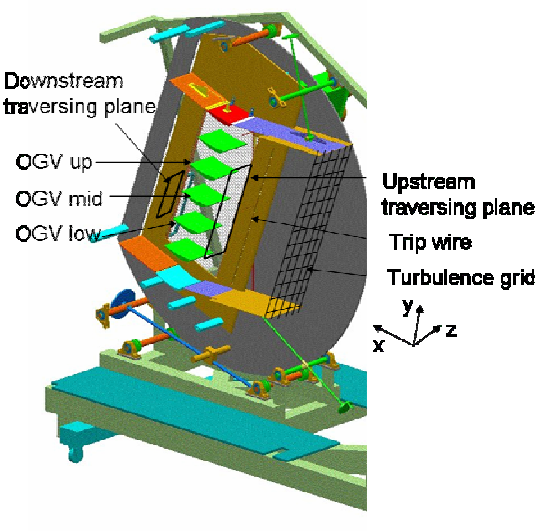

Figure 1 Drawing of the experimental set up.

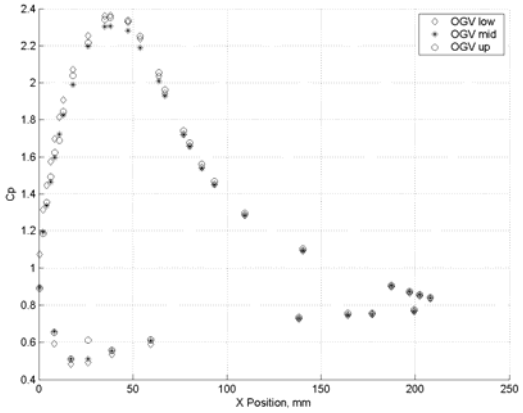

Figure 2 Cp distributions for the three mid OGV for the inlet flow angle 30 degrees and a turbulence intensity of 5%.

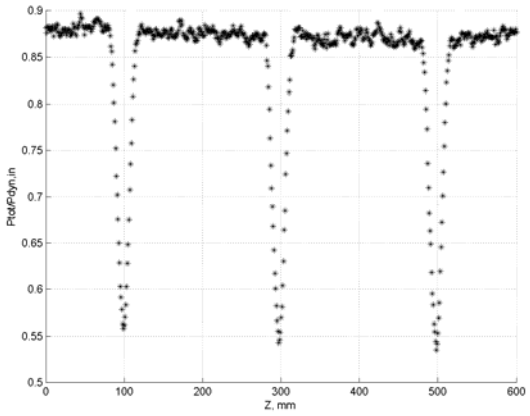

Figure 3 Downstream wakes of the total pressure (normalized with inlet dynamic head) for the on design case with a turbulent intensity of 5%.

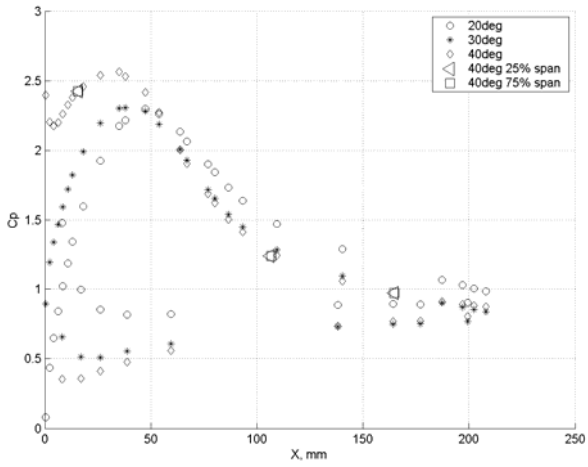

Figure 4 Cp distributions for the three different inlet flow angles

Instrumentation

Two traversing systems have been used to measure the flow field both upstream and downstream. The movements in the (y, z) plane are controlled by stepper motors with an accuracy of at least 12.5µm. The five hole pressure probes used for the upstream and downstream traverses have been manufactured at Chalmers and were calibrated between –20 to 20 degrees for both pitch and yaw angles. The finite size of the probe head diameter was 3.5 mm with an individual distance between the holes of 2 mm.

The inlet measurements were conducted 1.3*C upstream of the cascade with a discretization of 20mm in y and z direction. The typical total pressure variation was below 2% of the dynamic head. The upstream traversing system, equipped with a hot wire, was also used to measure the incoming boundary layer height along the side walls. In order to obtain a boundary layer height similar to what is present in a real engine, the end wall boundary layers were tripped with a 1.5 mm wire placed 1.36*C in the flow direction in front of the blade leading edge plane. The heights of the turbulent boundary layers (δ_{099}) were 9.6mm and 7.15mm respectively with and without the turbulence grid inserted. The boundary layers were measured in the flow direction 0.91*C upstream of the leading edge plane.

The downstream traversing system can be moved manually in the x direction with an accuracy of ± 0.0025*C. As the test rig has very good symmetry, see Hjärne et al. [8], the outlet measurements were taken over half of the span one pitch length over the central blade at three different streamwise locations downstream of the trailing edge (0.25*C, 0.5*C and 0.8*C). A discretization of 2mm in each direction was used. To avoid wall proximity effects, as suggested in [9], the flow field was not measured at a distance lower than two times the probe head size from the endwall.

3 RESULTS AND DISCUSSION

Complete investigations of an OGV downstream passage have been made with a 5-hole pressure probe. A time mean value of the flow field variables can thus be deduced. Besides the losses and outlet flow angles, by employing a high plane discretization, it was possible to compute the streamwise

vorticity. Even if it allows for a better understanding of the development of the secondary flows than the distributed total pressure losses, the interpretation of the results requires caution. There are multiple reasons for this. The first being that the probe has a finite head size with respect to the vorticity field. Secondly, the probe calibration is normally dependent on the turbulence intensity and anisotropy. Gregory-Smith and Cleak [2] have measured turbulence intensities up to 30 % in the loss core, which, from [9], can lead to an uncertainty on the measured pressure of 3%. Finally, pressure measurements do not resolve the time variation of the flow. These factors have an influence on the measured absolute value but this should not affect a global interpretation. It should also be noticed that the color scale used for plotting the results varies for each of the different inlet flow angles. This has been done to improve the resolution of the vorticity distribution in each case. For all the vorticity figures the pressure side points towards the top and the suction side towards the bottom, the sidewall standing on the left. To provide a better idea of what is happening within the flow, streamlines of the v- and w-components have been superimposed on the vorticity plots. In addition the maximum and minimum values for the positive and negative vorticity fields are shown at the top of each plot.

30deg inlet flow angle (design point)

Streamwise vorticity for the on design case (inlet flow angle 30 degrees) is presented in Fig. 5 and 6. Figure 5 represents the vorticity distribution with a turbulence intensity of 5% at 0.25*C, 0.5*C and 0.8*C going from left to right and the results for the lower turbulence intensity are shown in Fig. 6.

At a downstream position of 0.25*C in Fig. 5 a concentrated negative vorticity field occurs beneath the trailing edge close to the endwall. This circulation is clockwise as confirmed by the streamlines and will be referred to as the passage vortex even though it is hard to see from the streamlines if it actually is a vortex. Below this is the skewed boundary layer vorticity, also visible in blue, along the endwall growing from pressure side to suction side. It is obvious from the streamlines that the pressure gradient is pushing the endwall boundary layer towards the suction side and feeds the passage vortex. The final major visible vortical structure is the extended red area which is referred to as the blade shed vorticity. This vorticity is produced by the shedding motion of the fluid towards the OGV which is pushed away from the wall through interaction with the passage vortex. The absolute maximum intensity of the blade shed vorticity is higher compared to that of the passage vortex.

The relative evolution of these vorticity fields is depicted in the two following plots (Fig.5). The passage vortex core seems to remain at the same position, even if its strength is gradually decreasing. At the positions 0.5*C and 0.8*C downstream of the trailing edge, the passage vortex is not well defined since it has dissipated and merged together with the boundary layer vorticity. The boundary layer extends and decreases in intensity as the distance from the trailing edge increases. Considering the blade shed vorticity, it seems to roll up into a vortex which moves slightly towards mid span but remains at the same pitchwise position. This effect is depicted by the line A-A which is drawn through the locus of the blade shed vorticity field for all three downstream positions.

The result for the lower inlet turbulence intensity is shown in Fig. 6. The endwall boundary layer vorticity field appears to be thinner which results in an increased vorticity concentration compared to that seen in the higher inlet turbulence case. The relative differences seen in the properties of the blade shed vorticity and the passage vortex are linked to the features of the inlet boundary layer where the higher vorticity content is directly related to the higher inlet boundary layer vorticity concentration. The locus of the passage vortex has also got a higher intensity and is penetrating the blade shed vorticity to a larger extent. The blade shade vorticity consists of three smaller loci as highlighted in Fig 6 at downstream position 0.25*C. These legs merge together and evolve to form a vortex at 0.8*C. The effect of the higher turbulence intensity seems to mainly ensure an increased coherence of the vortical structures since dissipation has a more significant role.

The loading for an OGV is very much lower (less turning) compared to the turbine blades studied by the before mentioned authors [1-6]. In addition, the measurements presented in this paper are taken quite far downstream the trailing edge, and as a result the smaller structures mentioned by these authors have already dissipated. This explains why the resemblance with the theoretical model described by Wang et al. [4] for example, is poor.

20 degrees inlet flow angle (-10º incidence)

In Fig. 7 and 8 the downstream evolution of the streamwise vorticity for the lowest inlet angle is shown. Fig. 7 represents the higher turbulence intensity case and Fig. 8 the lower turbulence intensity case.

When the inlet flow angle decreases, the loading of the vane also decreases, and an interesting effect of this is that the passage vortex is barely visible in this case. The most probable explanation of this is that it has mostly dissipated at 0.25*C behind the trailing edge. A small dark blue spot is seen beneath the trailing edge close to the end wall and this is the only remaining evidence of the passage vortex. For this inlet flow angle the most visible vorticity fields are the boundary layer vorticity and the blade shed vorticity. The streamlines within the boundary layer vorticity field are still moving from pressure side to suction side, but because of the low loading, the blade shed vorticity dominates the flowfield. The downstream development is shown in the following two plots and is contrary to the on design case as the blade shade vorticity does not roll up into a vortex, instead it dissipates and dies out. The boundary layer vorticity field has the same evolution as for the on-design case, it becomes somewhat thicker but its intensity decreases.

In the low turbulence intensity case depicted in Fig. 8 similar evolutions are found. The blade shed vorticity is the most dominating part and the passage vortex is again very weak. In the same way as for the higher turbulence intensity, this vorticity dissipates and dies out at the furthest downstream position. The boundary layer vorticity increases its thickness but decreases its intensity.

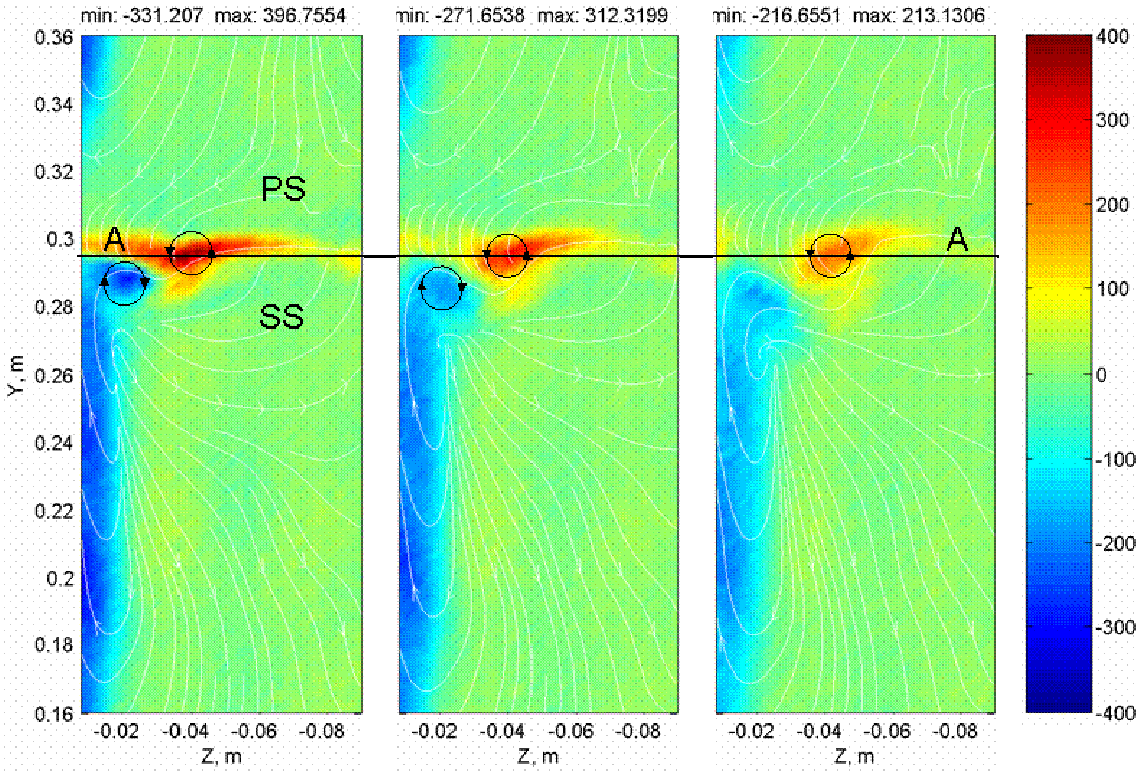

Figure 5 Streamwise vorticity for the on design case (inlet flow angle 30º) plotted downstream at positions 0.25*C, 0.5*C and 0.8*C with the turbulence intensity 5%. The view is aft looking forward.

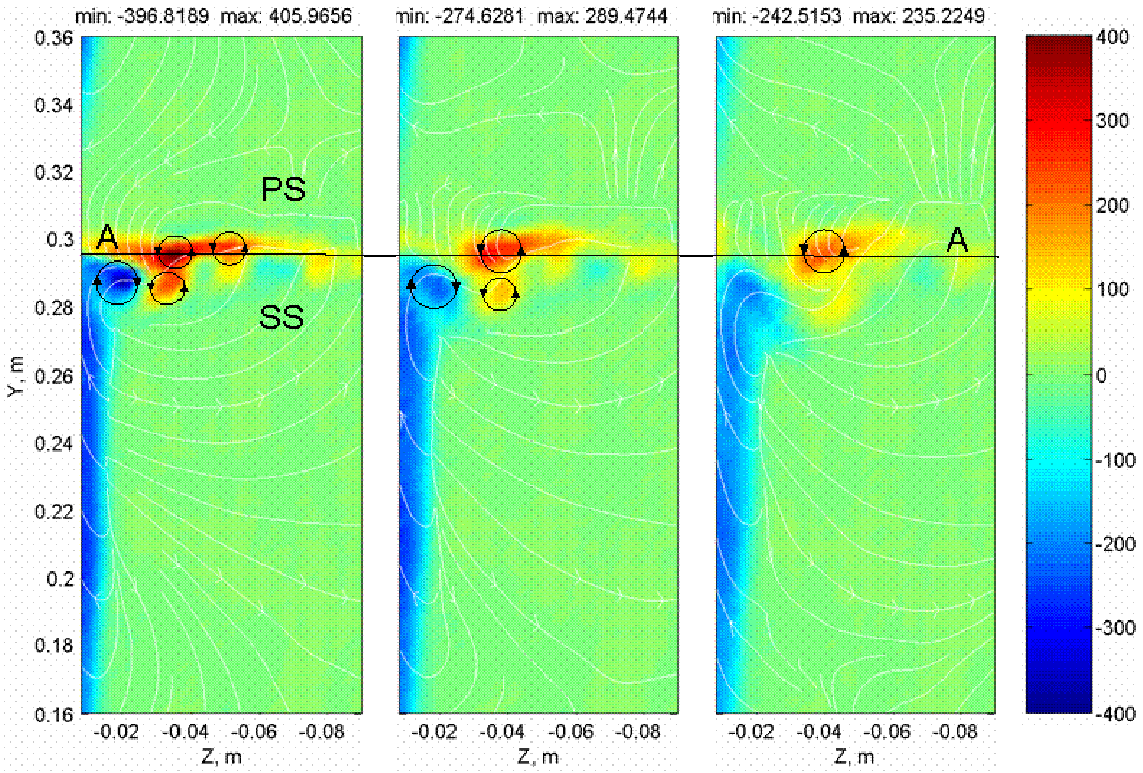

Figure 6 Streamwise vorticity for the on design case (inlet flow angle 30º) plotted downstream at positions 0.25*C, 0.5*C and 0.8*C with the turbulence intensity 0.5%. The view is aft looking forward.

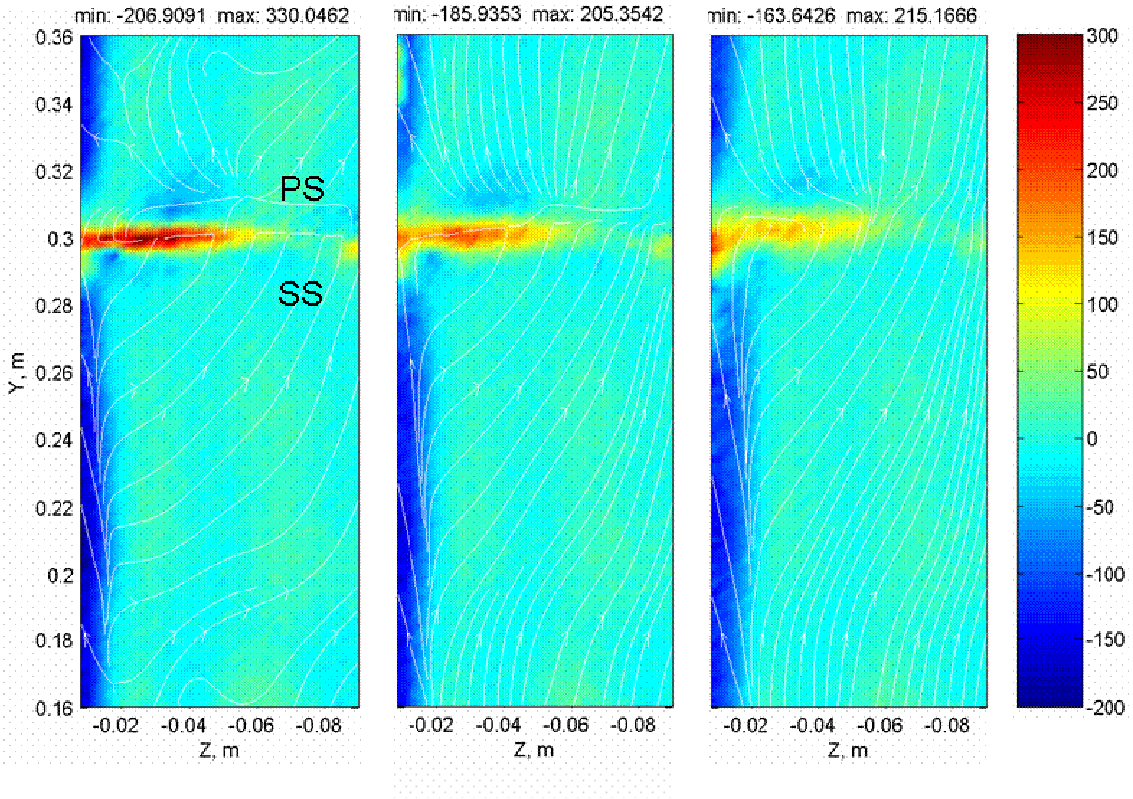

Figure 7 Streamwise vorticity for the inlet flow angle 20º plotted downstream at positions 0.25*C, 0.5*C and 0.8*C with the turbulence intensity 5%. The view is aft looking forward.

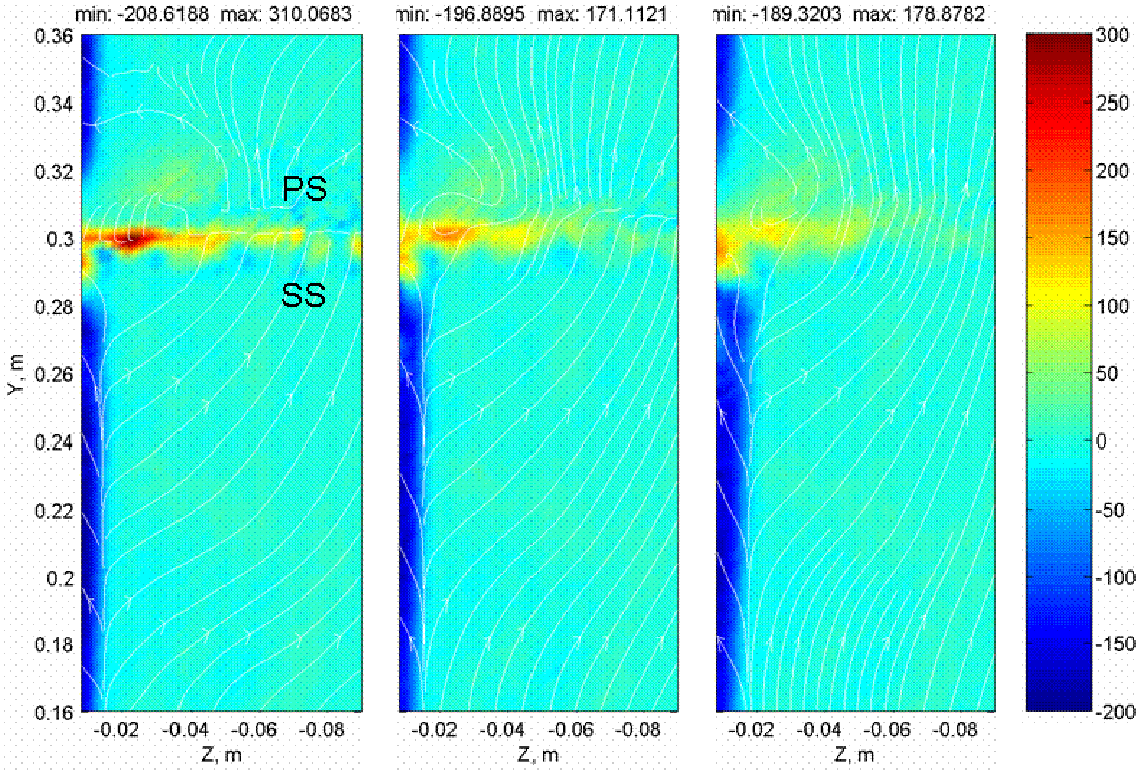

Figure 8 Streamwise vorticity for the inlet flow angle 20º plotted downstream at positions 0.25*C, 0.5*C and 0.8*C with the turbulence intensity 0.5%. The view is aft looking forward.

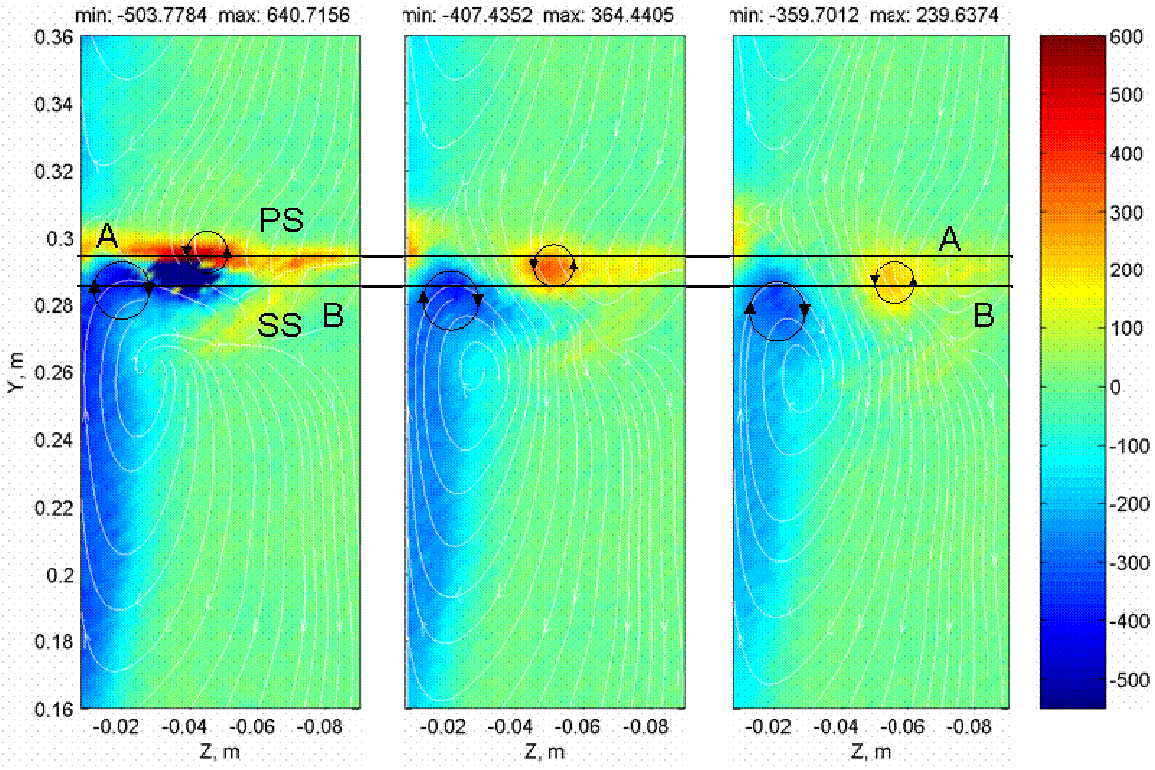

Figure 9 Stream wise vorticity for the inlet flow angle 40º plotted downstream at positions 0.25*C, 0.5*C and 0.8*C with the turbulence intensity 5%. The view is aft looking forward.

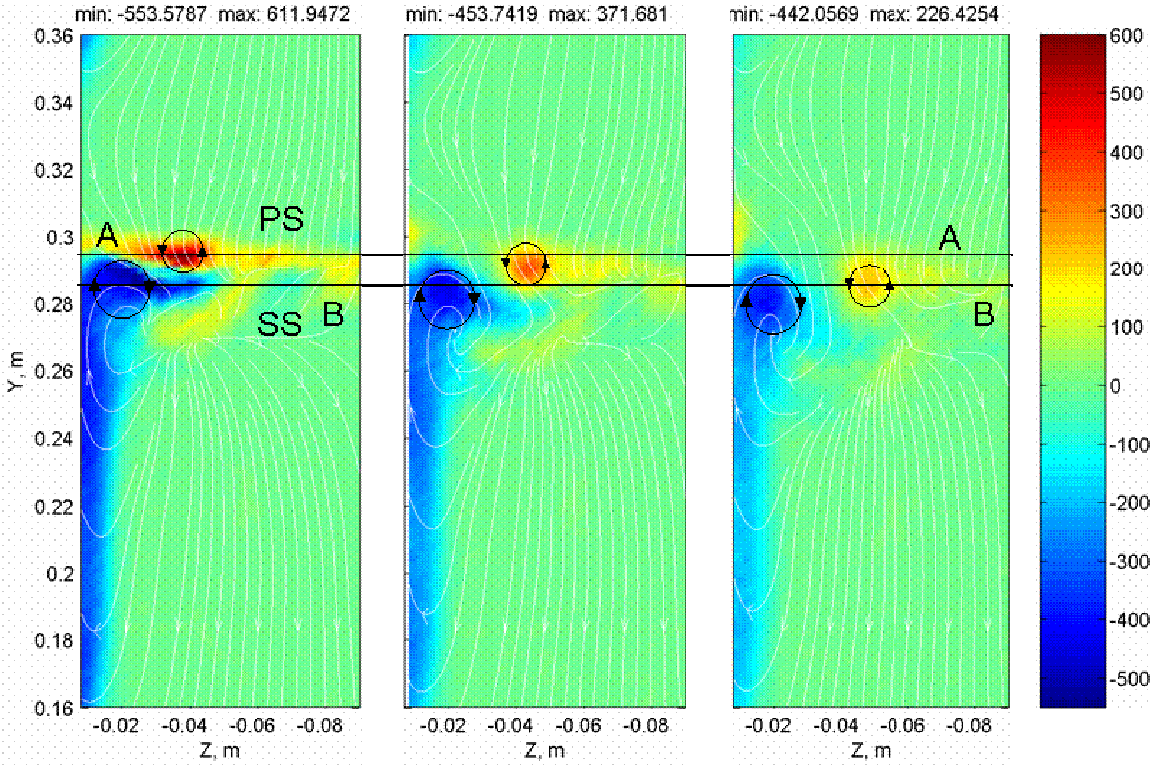

Figure 10 Stream wise vorticity for the inlet flow angle 40º plotted downstream at positions 0.25*C, 0.5*C and 0.8*C with the turbulence intensity 0.5%. The view is aft looking forward.

40 degrees inlet flow angle (+10º incidence)

The blade loading increases as the inlet flow angle changes to 40 degrees. The magnitude of the adverse pressure gradient on the blade rear suction side is enhanced and the transverse pressure gradient from pressure to suction side is increased. These combined effects influence the crossflow magnitude as well as the secondary flows strength, size and position. This situation is depicted in Fig. 9 for the high inlet turbulence intensity and Fig. 10 for the low turbulence intensity.

The passage vortex is bigger but still located close to the endwall. However, it is penetrating the blade shed vorticity more compared to that seen in the lower loadings at the closest downstream position 0.25*C. The intensity of the passage vortex has increased significantly compared to the lower loadings. In the downstream evolution of the boundary layer and the passage vortex, it is clear that as a results of the higher loading, the boundary layer is now feeding the passage vortex to a larger extent. This results in the boundary layer vorticity becoming thinner and its vorticity feeding the passage vortex to roll up into a vortex which extends almost to 25% of the whole outlet area.

Going further downstream some interesting effects occur. The locus of both the passage vortex and the blade shade vortex are now moving pitchwise. Because of the high loading, the OGV is not able to effectively turn the flow into an axial outflow, and as a result it can be seen that the v-velocity component increases and hence pushes the vortices towards the pressure side. This is clearly seen by looking at the plotted velocity components and the inserted lines A-A and B-B. The absolute value of the intensity of the passage vortex is also higher than the blade shed vortex for position 0.5 and 0.8*C. For the lower loadings the situation was that the absolute intensity of the blade shed vorticity generally was higher compared to that in the passage vortex. The effects which occur for this inlet flow angle are more comparable to a turbine blade than that seen in the lower loadings.

The result of the lower turbulence intensity is shown in Fig. 10. As for the two lower angles, the boundary layer becomes thinner but more intense when the turbulence intensity is decreased. The flow patterns are mainly the same as for the higher turbulence intensity.

4 LOSSES

The spanwise total pressure loss distributions for the different downstream positions are plotted in Fig 11-14. The losses are calculated as the mass averaged value of total pressure difference between the free stream and the total outlet divided by the inlet dynamic head.

30 deg inlet flow angle and different downstream positions

The high inlet turbulence intensity case shown in Fig. 11 has several interesting characteristics. Firstly, the value of the losses does not vary with the downstream distance from span position -0.065 to -0.09. It seems that no mixing but only dissipation takes place at this position. Then, the passage vortex together with the boundary layer leads to an increased value of the losses close to the endwall. Finally, the blade shed vorticity loss core induces a bump in the loss distributions which appears around -0.04 span locations. The variation in the loss distribution is directly related to the mixing process increasing with downstream position, whilst the migration of the secondary flow towards midspan is responsible for the "bump" seen in the distribution.

By comparison with the low inlet turbulence intensity case of Fig. 12, some differences can be found. Close to the endwall, the boundary layer vorticity and the passage vortex do not extend as long towards mid span which leads to a faster loss decrease. Closer to midspan, the blade shed vorticity loss bump is followed by a second one. The later of these two is linked to the lower turbulence intensity being responsible for the decreased coherency of the vortical structures.

Inlet flow angle effect on downstream losses

Figures 13 and 14 show the losses for various inlet flow angles at the furthest downstream plane, with and without turbulence grid respectively. At high inlet turbulence, the change of pattern from 20 to 30 degrees is linked to the secondary flow evolution. For the lowest loading the passage vortex has died out at this downstream position and does not push the blade shed vorticity away from the wall. In addition the blade shed vorticity has almost vanished because of dissipation and consequently the losses are low in this case. For the highest inlet flow angle the passage vortex extends a lot further from the endwall and concentrates into a vortex. The blade shed vorticity increases in size and strength and moves to midspan where it could start interacting with the opposite one. It is also clear that a higher loading has a strong impact on the level of losses. The high loss for this inlet flow angle is also linked to the suction side endwall corner separation. This separation is spread towards mid span which increases the losses significantly.

The low turbulence intensity case depicted in Fig 14 shows a similar spanwise loss evolution. One major difference for the lowest inlet flow angle is that the losses plateau over a wide part of the span. This contrasts with the evolution seen in the high inlet turbulence case and the difference is thought to again be related to the decreased coherency of the vortical structures when the turbulence intensity is low.

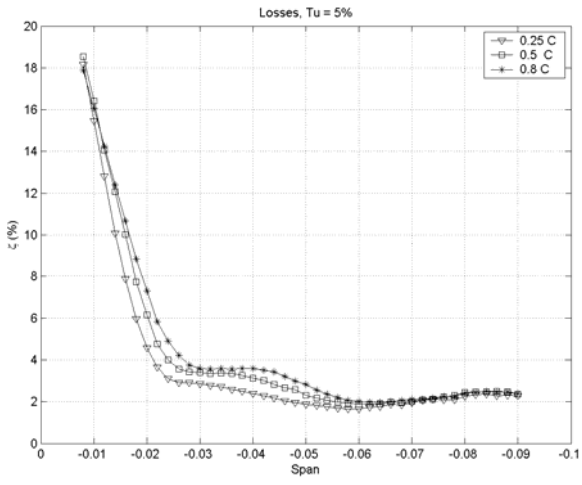

Figure 11 Losses for an inlet flow angle of 30 deg and Tu=5% at varying positions downstream

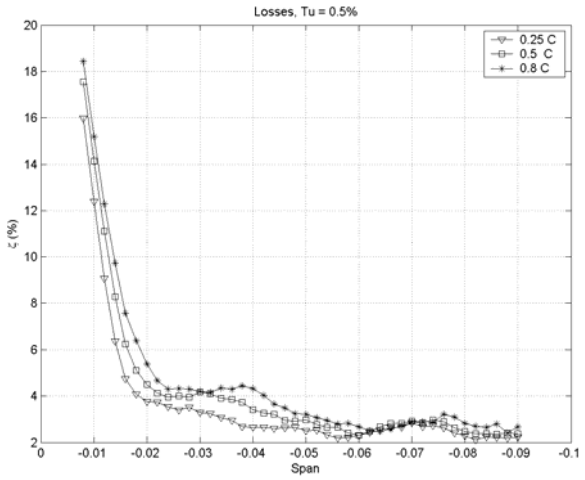

Figure 12 Losses for an inlet flow angle of 30 deg and Tu=0.5% at varying positions downstream

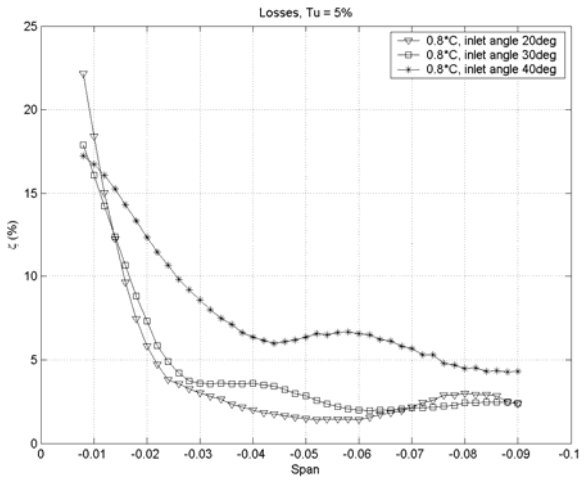

Figure 13 Losses for different inlet flow angles at the same downstream position 0.8*C and Tu=5%

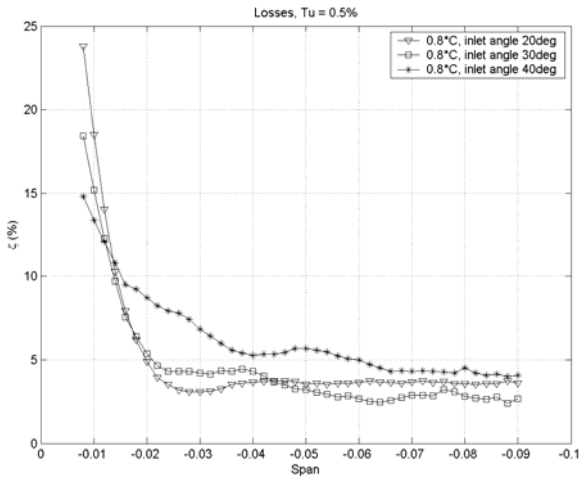

Figure 14 Losses for different inlet flow angles at the same downstream position 0.8*C and Tu=0.5%

5 CONCLUSIONS

This paper presents detailed experimental results for incidence and turbulence effects on three dimensional flows downstream of a LPT/OGV linear cascade. In addition to this the consequences of some boundary layer characteristics are also investigated. The results are summarized below.

- A good explanation of the downstream secondary flow field distribution can be developed from measurements of a 5-hole probe. The position, size and interactions of the main vortical structures are clearly visible and can be interpreted.
- The loading has an effect on the secondary flow intensity, the relative position of the developed vortical structures and their absolute location.
- The turbulence intensity enhances the coherency of the vortical structures and their mutual interactions. Its limited influence on the mean flow field characteristics reduces as the turning increases.
- For the same overall vorticity content and shape factor, the thickness of the inlet boundary layer influences the secondary flows position and size. The vorticity concentration within the inlet boundary layer has an impact on the downstream vorticity magnitude.

As shown by Gregory-Smith and Cleak [2], additional information could be provided for the downstream flow field with cross wires measurements.

ACKNOWLEDGEMENTS

The present work is a part of the project COOL supported by the Swedish Gas Turbine Center (GTC), and funded by Siemens, Volvo Aero Corporation and Energimyndigheten. The permission for publication is gratefully acknowledged. Special thanks also to PhD student Régis Houtermans at the Von Karman Institute for Fluid Dynamics for several valuable discussions and assistance with the experiments.

REFERENCES

[1] Sieverding, C. H., 1985 “Recent Progress in the Understanding of Basic Aspects of Secondary Flows in Turbine Blade Passages,” Transactions of the ASME, Vol. 107

[2] Gregory-Smith, D. G. and Cleak, J. G. E, 1992 ”Secondary Flow Measurements in a Turbine Cascade With High Inlet Turbulence,” Journal of Turbomachinery, Vol. 114

[3] Sharma, O. P. and Butler, T. L., 1987 ”Prediction of Endwall Losses and Secondary Flows in Axial Flow Turbine Cascades,” Journal of Turbomachinery, Vol. 109

[4] Wang, H. P., Olson, S. J., Goldstein, R. J. and Eckert, E.R.G., 1997 “Flow visualization in a Linear Turbine Cascade of High Performance Turbine Blades,” Journal of Turbomachinery, Vol. 119

[5] Goldstein, R. J. and Spores, R. A., 1988 “Turbulent Transport on the Endwall in the Region Between Adjacent Turbine Blades,” Transactions of the ASME, Vol. 110

[6] Kawai, T., Shinoki, S. and Adachi, T., 1990 “Visualization Study of Three-Dimensional Flows in a Turbine EndWall Region,” JSME International Journal, Series II, Vol. 33, No. 2

[7] Hjärne, J., Larsson, J. and Löfdahl, L., 2003, “Design of a Modern Test-Facility for LPT/OGV flows,” ASME paper GT2003-38083

[8] Hjärne, J., Larsson, J. and Löfdahl, L., 2005, “Experimental Evaluation of the Flow Field in a State of the Art Linear Cascade with Boundary-Layer Suction,” ASME paper GT2005-68399

[9] Arts, T., Boerrigter, H., Buchlin, J.-M., Carbonaro, M., Degrez, G., Dénos, R., Fletcher, D., Olivari, D., Riethmuller, M.L., Van den Braembussche, R.A., “Measurement Techniques in Fluid Mechanics”, 2nd revised edition, reprint of VKI LS 1994-01.

[10] Praisner, T.J., Smith, C.R., 2005, “The Dynamics of the Horseshoe Vortex and Associated Endwall Heat Transfer, Part I – Temporal Behavior”, ASME paper GT2005-66048.